

Spatiotemporal Growing Wave Fronts in Spatially Stable Boundary Layers

T. K. Sengupta,* A. Kameswara Rao, and K. Venkatasubbaiah

Department of Aerospace Engineering, I. I. T., Kanpur 208 016, India

(Received 27 February 2006; published 8 June 2006)

In fluid dynamical systems, it is not known *a priori* whether disturbances grow either in space or in time or as spatiotemporal structures. For a zero pressure gradient boundary layer (also known as the Blasius boundary layer), it is customary to treat it as a spatial problem, and some limited comparison between prediction and laboratory experiments exist. In the present work, the two-dimensional receptivity problem of a Blasius boundary layer excited by a localized harmonic source is investigated under the general spatiotemporal framework, by using the Bromwich contour integral method. While this approach is seen to be equivalent to the spatial study for unstable systems, here we show for the first time how spatially stable systems show spatiotemporally growing wave fronts.

DOI: 10.1103/PhysRevLett.96.224504

PACS numbers: 47.20.Pc, 47.15.Fe, 47.20.Ib

Hydrodynamic stability theory aims to link laminar and turbulent flows. Despite significant advances made [1,2], there are still issues of transition that remain incompletely understood. Classical approaches to instability studies identify an equilibrium state, whose stability is studied by eigenvalue analysis by linearizing the governing equations. This analysis seeks the least stable eigenmode, for parallel flows, of the linearized Navier-Stokes equation in the spectral plane [giving the Orr-Sommerfeld equation, as given by Eq. (2)] whose solution exhibits waves for particular parameter combinations, and these are known as the Tollmien-Schlichting (TS) waves. The Reynolds number (Re) at which the equilibrium flow first becomes unstable for any harmonic excitation is the critical Reynolds number (Re_{cr}).

Results obtained by this approach match with laboratory experiments for thermal and centrifugal instabilities. Instabilities dictated by shear force do not match as well, e.g., (i) Couette and pipe flows are found to be linearly stable at all Re , while the former is known to suffer transition at $Re = 350$ and the latter at $Re \geq 1950$ [3] in laboratory experiments, with the exact value dependent upon facilities and background noise level; (ii) plane Poiseuille flow has a $Re_{cr} = 5772$, whereas in experiments transition was seen to occur at $Re = 1000$ [4]. According to Ref. [3], even for Blasius boundary layer, success of eigenvalue analysis is of a lesser degree.

The above discrepancies of linear stability theory in not being able to predict the subcritical transition have prompted many to seek alternatives in nonlinear theories [5,6], secondary instabilities [7], etc. In recent times, the failure of eigenvalue analysis has been attributed to analysis methods, and, instead, subcritical transition is attributed to *nonorthogonal* or *non-normal* eigenvectors that can cause large transient energy growth [8,9] for stable systems. One of the features of this nonmodal amplification is that it applies to three-dimensional perturbation only [3].

In the present work, an overlooked aspect of linearized analysis is highlighted to account for subcritical transition. Usual eigenvalue analysis treats it as either a spatial or a

temporal problem. Specially, spatial stability is used for velocity profiles without inflection points, as for the Blasius boundary layer. This has been established by receptivity analysis [10], where the problem shown schematically in Fig. 1 was solved for the Blasius boundary layer excited by a harmonic localized source. The non-dimensional disturbance stream function (ψ) was obtained from the Bromwich contour integral [11,12],

$$\psi(x, y, t) = \frac{e^{-i\beta_0 t}}{2\pi} \int_{Br} \phi(y, \alpha, \beta_0) e^{i\alpha x} d\alpha, \quad (1)$$

where β_0 is the circular frequency of excitation and Br indicates the Bromwich contour followed in evaluating the above integral in the complex wave-number (α) plane. This is the signal problem where the transient part of the solution is not considered and time dependence is harmonic. In the present formulation, all the lengths have been nondimensionalized by the displacement thickness (δ^*) of the boundary layer that characterizes the effect of mass defect by viscous action at the wall. All velocities are nondimensionalized by the free-stream velocity (U_∞) and time by δ^*/U_∞ . The bilateral Laplace transform ϕ defined in (1) is obtained as a solution of the Orr-Sommerfeld equation [1],

$$\left[U(y) - \frac{\beta_0}{\alpha} \right] (\phi'' - \alpha^2 \phi) - U'''(y) \phi = \frac{(\phi^{iv} - 2\alpha^2 \phi'' + \alpha^4 \phi)}{i\alpha Re}, \quad (2)$$

where U is the parallel equilibrium flow taken at the location of the exciter, which is equivalent to taking the shear layer to be parallel, as indicated in Fig. 1. In the above, primes indicate derivatives with respect to y and $Re = U_\infty \delta^*/\nu$, with ν as the kinematic viscosity. In Ref. [10], the Bromwich contour was taken as parallel and below the real α axis, such that all the downstream propagating modes are above this line. In this receptivity approach, effects of all the modes are incorporated, which

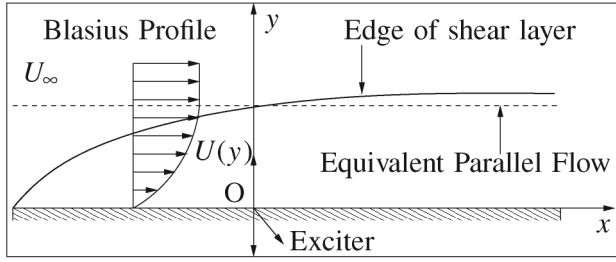


FIG. 1. Harmonic excitation of a parallel boundary layer corresponding to the location of the exciter.

is in contrast to normal mode eigenvalue analysis that tries to explain everything in terms of the leading eigenmode only.

In the signal problem [10], the implicit assumption that the response is at the frequency β_0 of the exciter may not seem as drastic. But for absolute unstable systems, initial transient associated with startup can fix the response at the absolute frequency that is, in general, different from β_0 . In Ref. [13], an attempt was made to obtain a criterion whereby flows could be analyzed by either the spatial or the temporal theory—overlooking the possibility of simultaneous spatiotemporal response. We show here that the latter is of prime importance for spatially stable systems.

In Ref. [14], spatiotemporal theory was used to ascertain the inviscid instability of jets and wakes and to estimate the characteristic frequency of the response. Similarly, in Refs. [15,16], the receptivity problem of wave-packet propagation created by a single pulse was studied in the context of a stationary phase asymptotic solution obtained by the saddle point method. In contrast to these spatiotemporal approaches, in Ref. [17] a complete spatiotemporal problem was studied, without the assumption of the signal problem, where ψ was obtained from

$$\psi(x, y, t) = \frac{1}{(2\pi)^2} \iint_{\text{Br}} \phi(\alpha, \beta, y) e^{i(\alpha x - \beta t)} d\alpha d\beta \quad (3)$$

and ϕ obtained from the solution of Eq. (2) (with β_0 replaced by β) along the Bromwich contours in the complex α and β planes. The choice of Bromwich contours in the β plane is restricted by causality, and the contour in the α plane is similar to that used in Refs. [10,17]. In the following, Cartesian disturbance velocity components are denoted by u and v , respectively. Therefore, for the excitation shown in Fig. 1, boundary conditions at $y = 0$ are $u = 0$, $\psi(x, 0, t) = H(t)\delta(x)e^{-i\beta_0 t}$ and for $y \rightarrow \infty$: $u, v \rightarrow 0$, where $H(t)$ is the Heaviside function and $\delta(x)$ represents the Dirac delta excitation at the origin of the frame. The conclusion [17] was that, for a spatially unstable case ($\text{Re} = 1000$ and $\beta_0 = 0.1$), the evolving solution has the same parameters as that obtained in Ref. [10]; i.e., the space-time dependent solution is determined mainly by the unstable eigenvalue, with the damped modes playing no role. The results presented in Ref. [17] were for a spatially unstable case only and not undertaken for stable

cases. This is investigated here, specifically to look for spatiotemporal growing solutions that are otherwise spatially stable.

To discuss the spatiotemporal growth of waves for the Blasius boundary layer, a few cases are considered marked as A, B, C, and D in Fig. 2, with respect to the neutral curve shown in the $(\text{Re}-\beta_0)$ plane, for the leading eigenmode. A neutral curve demarcates stable and unstable regions of the $(\text{Re}-\beta_0)$ plane—as indicated in this figure. The Bromwich contour for point A is chosen in the α plane on a line extending from -20 to $+20$ that is below and parallel to the α_{real} axis at a distance of 0.009, and in the β plane it extends from -1 to $+1$ above and parallel to the β_{real} axes at a distance of 0.02. For the other points, the Bromwich contour in the α plane is located at a distance of -0.001 from the α_{real} axis. The choice of Bromwich contour in the α plane is such that all the downstream propagating eigenvalues lie above it. Equation (2) has been solved along these contours with 8192 equidistant points in the α plane and 512 points in the β plane. In Ref. [17], results were reported for point A, with only half the number of points in the α and β planes and 1200 points were taken in $0 \leq y \leq 6.97$, as compared to 2400 points used here. An increase in the number of points is mandatory to obtain solutions valid over a longer domain and times. All other numerical details are the same as in Ref. [17]. Spatial stability analysis produces waves for the four points of Fig. 2 with the properties as given in Table I. For point A, receptivity analysis produces streamwise perturbation velocity (u) as shown in the bottom frame in Fig. 3 at $t = 801.1$. In Fig. 3, the top two frames show solutions for the case of point B. The present results obtained for point A are indistinguishable from the growing asymptotic solution obtained by signal problem analysis in Ref. [10]. This type of receptivity analysis provides additionally the local solution (in the neighborhood of the exciter), and a frontrunner (for B and not for A) preceding the asymptotic solution. It can be shown analytically that the local solution is due to the essential singularity of the α plane and numerically identified in Ref. [10]. For point A, the receptivity solution is determined by the first mode alone, without any effects coming from the second and third modes of Table I. In contrast, for point B, the asymptotic solution is due to the first mode of Table I (in terms of wavelength and decay rate) and the growing wave front corresponds to the second

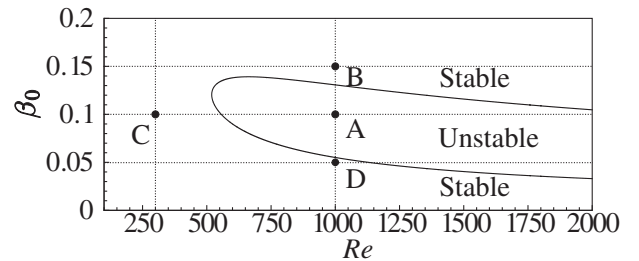


FIG. 2. Neutral curve for the Blasius boundary layer identifying stable and unstable regions.

TABLE I. Wave properties of selected points in Fig. 2.

Mode	α_r	α_i	V_g	V_s	V_e
A1	0.279 826	-0.007 287	0.4202	0.42	0.42
A2	0.138 037	0.109 912	0.4174
A3	0.122 020	0.173 933	0.8534
B1	0.394 003	0.010 493	0.4267	0.352	0.352
B2	0.272 870	0.167 558	0.2912		
B3	0.189 425	0.322 635	0.1159		
C1	0.246 666	0.013 668	0.5026	0.50	0.50
D1	0.160 767	0.001 520	0.3908	0.33	0.33
D2	0.062 141	0.069 659	0.2762		

mode, in terms of the wavelength. The effects of the third mode are not seen to contribute to the overall solution. It is noted that the leading edge of the asymptotic solution continues to decay at the same rate predicted by the spatial eigenvalue analysis, while the frontrunner continues to grow spatiotemporally, although the spatial theory identifies this as a damped mode.

The necessary condition for the creation of a frontrunner can be found by looking at the receptivity solutions for points C and D, with the former having a single stable mode and the latter with two damped modes. Results for u are shown in Fig. 4 at the indicated time. The essential difference between these and previous cases in Fig. 3 is that the latter have three modes, while C possesses a single mode and D possesses two modes. The frontrunner in Fig. 3 is due to interactions of multiple stable modes. In the absence of multiple modes—as for point C—no such frontrunner is seen in Fig. 4. Again, for point D, there are only two stable modes that create a spatiotemporally growing frontrunner. Thus, for fluid dynamical systems, the presence of a minimum of two stable modes is necessary to produce a spatiotemporally growing wave front, when the least stable mode is spatially damped.

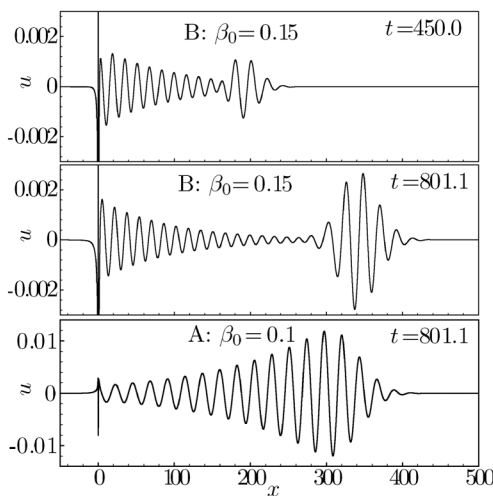


FIG. 3. Streamwise disturbance velocity (u) plotted as a function of x at indicated times for $Re = 1000$, $y = 0.278$.

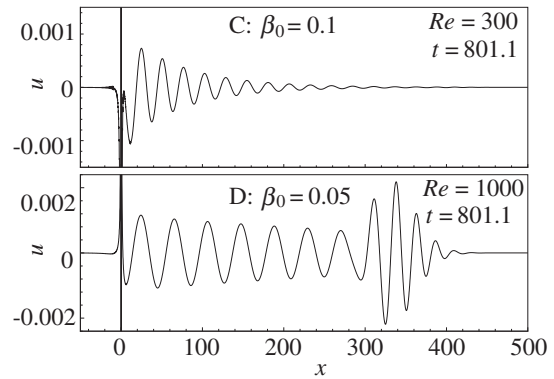


FIG. 4. u plotted as a function of x at indicated times for $Re = 300$ and 1000 for the indicated β_0 at $y = 0.278$.

The growth of the frontrunner is due to the competing groups associated with multiple stable modes, reinforcing each other at the front. What we have called here the frontrunner is also referred to as the *forerunner* in the literature [18]. The propagation of a wave front and forerunner in a material medium has been of continuing interest. The propagation speed has been variously described as the group velocity by Rayleigh, signal velocity by Sommerfeld, and also the velocity of energy transfer in Ref. [18]. It is noted [18] that the three definitions are identical for nondissipative systems. But, in dissipative systems, these can differ considerably. It is also shown [18] that the forerunner is very weak and difficult to trace for stable systems, and it can attain high amplitudes only when the group velocity attains a minimum. In the context of the present problem, group velocity (V_g) is obtained from eigenvalue analysis—as given in Table I. From Figs. 3 and 4, one directly estimates the signal velocity (V_s) by tracking the crests, as shown in the second last column of Table I. In the following, an estimate for the energy propagation speed (V_e) is obtained.

If the total mechanical energy of incompressible flow is identified as $E = p/\rho + V^2/2$, then the evolution of disturbance energy can be studied following the method of Ref. [19], where the disturbance energy (E_d) is calculated

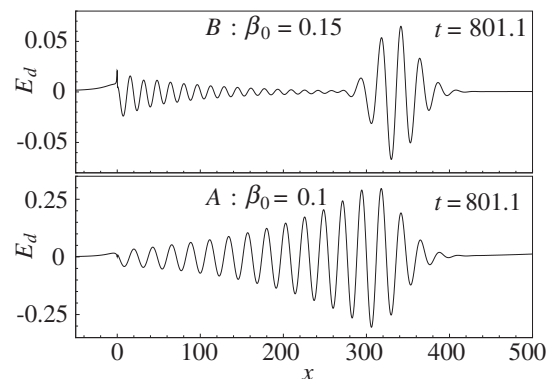


FIG. 5. Disturbance energy (E_d) plotted as a function of x at indicated times for $Re = 1000$, $y = 0.278$.

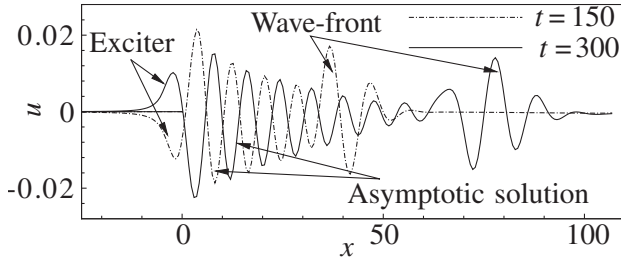


FIG. 6. u vs x at $y = 0.648$ obtained by solving the Navier-Stokes equation for simultaneous blowing-suction excitation at the wall for $Re = 1000$, $\beta_0 = 0.14$.

from

$$\nabla^2 E_d = \nabla \cdot (V_m \times \omega_d) + \nabla \cdot (V_d \times \omega_m), \quad (4)$$

with V and ω representing velocity and vorticity field, respectively, and the subscripts m and d identify equilibrium and disturbance quantities, respectively. If one represents E_d in terms of its Fourier-Laplace transform via $E_d(x, y, t) = [1/(2\pi)^2] \iint_{Br} \hat{E}_d(y) e^{i(\alpha x - \beta t)} d\alpha d\beta$, then the governing equation for \hat{E}_d is given by

$$\begin{aligned} \hat{E}_d'' - \alpha^2 \hat{E}_d &= \phi''' U + 2\phi'' U' + \phi'(U'' - \alpha^2 U) \\ &\quad - 2\phi \alpha^2 U'. \end{aligned} \quad (5)$$

We solved Eq. (5) for \hat{E}_d as a function of α and β and reconstructed E_d as a function of x and t by performing Bromwich integrals successively. Results for E_d are shown as a function of x for points A and B in Fig. 5. E_d shows smoothly decreasing variation, upstream of the exciter. Also, E_d is less spiky as compared to u at the location of the exciter. Once again, for point A , there is no frontrunner, while point B displays the same as before. The rate at which E_d propagates can be estimated roughly from this figure. We note that the system dynamics is determined by the least stable mode ($A1$) for the spatially unstable case, with all three definitions of propagation speed producing identical results—as seen in Table I. In contrast, for stable systems with multiple modes, the frontrunner has identical V_s and V_e , which lies between the group velocity values of the leading two modes. For stable systems with a single mode, all three definitions produce the same value. Thus, for all systems the signal speed and energy propagation speed are the same.

The appearance and propagation of a frontrunner is not a transient phenomenon, and this can be further demonstrated by performing direct simulation of the 2D Navier-Stokes equation. The formulation and numerical method is as noted in Ref. [20], and typical results of a run are shown in Fig. 6, where the Blasius boundary layer is excited by a simultaneous blowing-suction source at the wall—a similar problem was solved in Ref. [21]. Results shown for $t = 150$ and 300 clearly identify the frontrunner. This verification is necessary, as the receptivity solutions are based on

parallel flow approximation, which does not account for the growth of the boundary layer.

We conclude by noting that a growing frontrunner is created as spatiotemporal perturbations in a spatially stable fluid dynamical system with multiple modes. For unstable systems, no such frontrunner is seen. This is also verified from the direct simulation of the 2D Navier-Stokes equation. This result could be of broad interest and contribute to the understanding of the long-standing discrepancies observed in some systems between the analytical results obtained using linear spatial stability theory and actual experimental observations on flow transition.

*Electronic address: tksen@iitk.ac.in

- [1] P.G. Drazin and W. Reid, *Hydrodynamic Stability* (Cambridge University Press, Cambridge, England, 1981).
- [2] P.J. Schmid and D.S. Henningson, *Stability and Transition in Shear Flows* (Springer-Verlag, New York, 2001).
- [3] L.N. Trefethen, A.E. Trefethen, S.C. Reddy, and T.A. Driscoll, *Science* **261**, 578 (1993).
- [4] S.J. Davies and C.M. White, *Proc. R. Soc. A* **119**, 92 (1928).
- [5] L.D. Landau, *Collected Papers* (Pergamon, Oxford, United Kingdom, 1965).
- [6] B. Hof, C.W.H.V. Doorne, J. Westerweel, F.T.M. Nieuwstadt, H. Faisst, B. Eckhardt, H. Wedin, R.R. Kerswell, and F. Waleffe, *Science* **305**, 1594 (2004).
- [7] B.J. Bayly, S.A. Orszag, and T. Herbert, *Annu. Rev. Fluid Mech.* **20**, 359 (1988).
- [8] K.M. Butler and B.F. Farrell, *Phys. Fluids A* **4**, 1637 (1992).
- [9] S.C. Reddy and D.S. Henningson, *J. Fluid Mech.* **252**, 209 (1993).
- [10] T.K. Sengupta, in *Proceedings of the 7th International Conference on Numerical Methods in Laminar and Turbulent Flows* (Pineridge Press, United Kingdom, 1991).
- [11] A. Papoulis, *The Fourier Integral and Its Application* (McGraw-Hill, New York, 1962).
- [12] B.V.D. Pol and H. Bremmer, *Operational Calculus Based on Two-Sided Laplace Integral* (Cambridge University Press, Cambridge, United Kingdom, 1959).
- [13] P. Huerre and P.A. Monkewitz, *J. Fluid Mech.* **159**, 151 (1985).
- [14] R. Betchov and W.O. Criminale, *Phys. Fluids* **9**, 359 (1966).
- [15] M. Gaster, *Phys. Fluids* **11**, 723 (1968).
- [16] A. Bers, *Physique des Plasmas* (Gordon and Breach, New York, 1975).
- [17] T.K. Sengupta, M. Ballav, and S. Nijhawan, *Phys. Fluids* **6**, 1213 (1994).
- [18] L. Brillouin, *Wave Propagation and Group Velocity* (Academic, New York, 1960).
- [19] T.K. Sengupta, S. De, and S. Sarkar, *J. Fluid Mech.* **493**, 277 (2003).
- [20] T.K. Sengupta, A. Guntaka, and S. Dey, *J. Sci. Comput.* **21**, 269 (2004).
- [21] H. Fasel and U. Konzelmann, *J. Fluid Mech.* **221**, 311 (1990).